MATCH
Communications in Mathematical and in Computer Chemistry

MATCH Commun. Math. Comput. Chem. **64** (2010) 391-418

ISSN 0340 - 6253

ON ABSOLUTE AROMATICITY WITHIN ELECTRONEGATIVITY AND CHEMICAL HARDNESS REACTIVITY PICTURES

Mihai V. Putz

Laboratory of Computational and Structural Physical Chemistry, Chemistry Department, West University of Timişoara, Str. Pestalozzi No. 16, Timişoara, RO-300115, Romania

Tel:+40-256-592633, Fax: +40-256-592620

E-mails: mvputz@cbg.uvt.ro, mv_putz@yahoo.com

Web: http://www.mvputz.iqstorm.ro

(Received December 22, 2009)

Abstract

The absolute aromaticity formulation based on the comparison between the pre-bonding stage of atoms-in-molecules and the post-bonding stage of molecular orbitals is advanced. The specialized electronegativity and chemical hardness- based absolute aromaticity indices are proposed within various computational schemes of compact finite differences of frontier orbitals up to the spectral-like resolution, with the scales trends established through their popular reactivity principles, respectively. The reliability of the obtained aromaticity scales was tested throughout the consecrated geometrical, topological, energetic (including thermodynamic), and magnetic criteria on a paradigmatic set of benzenoid hydrocarbons. The Mulliken electronegativity-based aromaticity scale was found to correlate best with exaltation of magnetic susceptibility, whereas for the chemical hardness the fashioned HOMO-LUMO gap description of aromaticity was improved towards its second and third order differences that prove superior agreement with aromaticity scales based on topologic analysis. The best correlations found in modeling the aromaticity criteria by the chemical hardness-based schemes of computations advocate considering further the associate hard-

and-soft acids-and-bases and maximum hardness principles as main tools for assessing chemical reactivity and molecular stability.

1. Introduction

The aromaticity concept and its evaluation has always been one of the oldest problems of chemistry that has yet to be solved. The subject has extended over almost two centuries since 1825, when Faraday discovered the so-called "bicarburet of hydrogen", then consecrated as benzene by Kekulé's 1865 works [1], who advanced the aromaticity phenomenon as being responsible for the observed extra-stability of certain cyclic non-saturated compounds.

The history of aromaticity is reach and exciting and among many pioneering contributions to its description, there are some worth remembering: for example, those of "three electrons in each CC region of benzene" of Thomson (in 1921) [2], then segregated into the σ-π quantum contributions by Hückel (in 1930) [3], and the thermal and photochemical rules of aromaticity and anti-aromaticity of Doering and Detert (in 1951) [4]; other specific structural properties such as continuous conjugation [5] and planarity [6] were initially admitted, then relaxed [7] even for the assumed planar referential aromatic molecule of benzene [8]. Recently, aromaticity has been extended to all metal molecules [9], emphasizing the geometrical and reactivity description as feasible tools for assessing its features.

As far the geometrical side is concerned, the CC bond length variation in the molecular area leads to the Julg and Françoise (1967) aromaticity index [10], whereas when improved by stereochemical optimization it produces the harmonic oscillatory model based aromaticity (HOMA) of Krygowski (in 1972, 1993) [11]. Instead, when combined with the resonance energy the so-called topological indices have been advanced for describing aromaticity through the conjugated circuits of Randić and simultaneously of Gutman et al. (in 1977) [12]; they have recently been generalized for accounting the limit Kekulé structures by the topological resonance energy index of Aihara et al. (in 2005) [13], or through introducing by Tarko (in 2008) of the aromatic range for the bond orders' values and the aromatic zones for the topological paths in what was called the topological paths and aromatic zones (TOPAZ) algorithm [14].

Going to the reactivity modeling of aromaticity, the fruitful direction of molecular topological description was ultimately employed to reflect an aromatic

electrophilic substitution reaction for the most favorable energetic position in a molecule by introducing the topologic index of reactivity (TIR) by Balaban et al. (in 1985, 2005, and 2008) [15].

On the other hand, by using the "primitive patterns of understanding" reactivity [16], the modern density functional electronegativity (χ) [17] and chemical hardness (η) [18] formulations as the first and second derivatives of the total (or valence) energy (E) of a system respecting the associate number of electrons (N) under constant potential influence $V(\mathbf{r})$

$$\chi = -\left(\frac{\partial E}{\partial N}\right)_{V(\mathbf{r})} \tag{1}$$

$$\eta = \frac{1}{2}\left(\frac{\partial^2 E}{\partial N^2}\right)_{V(\mathbf{r})} \tag{2}$$

have been related by Chattaraj et al. (in 2007) with aromaticity [19] in the light of their principles, especially those regarding Pearson's hard-soft-acid-base [20] and the maximum hardness [21] ones.

Yet, for most of these approaches, either energetic, geometric, reactivity, or of their combined pictures, the aromaticity concept is viewed in terms of a global or local index as the difference between its value for the structure under investigation and that observed/computed for some referential compound or state [22]. This seems natural since aromaticity is attributed the stability measure of a molecular sample – therefore providing a relative scale – a behavior considered by Katritzky et al. (in 1998, 2002) [23] as a "multidimensional characteristic".

In this context, the present approach makes one further step in assigning aromaticity an absolute framework based on electronegativity and chemical hardness molecular indices by replacing the *tested–to–referential molecule* difference with the *atoms in molecule–to–the same molecule's frontier orbitals* difference scheme of computation. Then, obtained aromaticity scales are to be compared with those based on various physico-chemical consecrated models.

2. Reactivity-Based Absolute Aromaticity

To introduce absolute aromaticity, two ways of expressing electronegativity and chemical hardness will be presented: one has its roots in the atoms-in-molecules

reactivity principles and the other employs their density functional definitions into the compact finite differences of frontier-orbitals energies of higher orders.

2.1. Electronegativity of Atoms in Molecule

Since the electronegativity is ultimately identified with the negative of the chemical potential because based on the same working definition – see eq. (1) [17a], its molecular level can be established within the reactivity picture in which the (valence) electronic (fluids) of the adduct samples are interchanged until the equalization of their separated chemical potential into the unique molecular one is established. This is the phenomenological base for what is known as the electronegativity equalization (EE) principle of atoms in molecule(s) (AIM) [24].

Quantitatively, the AIM electronegativity is generalized from the working formulation of the diatomic A-B molecule at equilibrium [17b,17c,18c,18e,24]

$$\chi_{AB} \equiv \overline{\chi} = \frac{\eta_A \chi_B + \eta_B \chi_A}{\eta_A + \eta_B} \tag{3}$$

that displays a sort of global chemical hardness normalization (at denominator) for the mixed terms of reciprocally combined electronegativity of one atom with the chemical hardness of the other in bonding (at nominator). Such shape of the equalized electronegativity of AIM has meaningful consequences in reactivity: (i) the denominator contribution shows that the molecular system is stabilized when the molecular electronegativity is minimized by the maximized chemical hardness, leading with the indirect necessity the chemical hardness is maximum for less reactive systems; (ii) the nominator contribution tells that the bonding may be modeled by the competition result between the two opposite tendencies of atomic reactivity, i.e. that coming from the propensity (electronegativity) of one atom (say A) on the electrons belonging to the partner B-atom, while being this action modulated by the resistance (the counter action) of the chemical hardness of the B-atom in bonding.

Yet, the form of eq. (3) is not susceptible to explicit generalization to many atoms in molecule, unless a close relation is obtained in atomic electronegativities only. This may be achieved through considering a sort of universal invariant θ that transforms electronegativity into the chemical hardness effect at whatever level of electronic complexity, atoms and molecules (here represented for paradigmatic *AB* bonding by χ_{AB} and η_{AB})

$$\chi_A = \theta\ \eta_A, \chi_B = \theta \eta_B, \chi_{AB} = \theta \eta_{AB} \tag{4}$$

Such transformation is formally justified by observing from eqs. (1) and (2) the general relationship between electronegativity and chemical hardness

$$\chi_{V(\mathbf{r})} = -2\int \eta[N]dN \tag{5a}$$

In turn, eq. (5a), rewritten within derivative fashion

$$\eta = -\frac{1}{2}\left(\frac{\partial \chi}{\partial N}\right)_{V(\mathbf{r})} \tag{5b}$$

is in agreement with the physical force-potential $F = -\nabla V$ paradigm of chemical reactivity: if electronegativity is equivalent with the minus of chemical potential, its further derivative behaves like the chemical force that is the chemical hardness.

Now, adopting the electronegativity – chemical hardness transformations of eq. (4) the AIM electronegativity of eq. (3) rewrites only with the atomic electronegativity contributions

$$\overline{\chi} = \frac{2}{\dfrac{1}{\chi_A} + \dfrac{1}{\chi_B}} \tag{6}$$

that permits the direct generalization to the polyatomic molecules [25]

$$\chi_{AIM} = \frac{n_{AIM}}{\displaystyle\sum_A \frac{n_A}{\chi_A}} \tag{7}$$

where the total atoms in molecule n_{AIM} is the sum of the n_A atoms of each A-species present in the molecule

$$\sum_A n_A = n_{AIM} \tag{8}$$

Of course, at this point one can immediately write down the companion AIM chemical hardness formulation by using the transformations of eq. (4) upon the AIM electronegativity of eq. (7). However, because of the ansatz nature of eq. (4) we prefer to derive separately the AIM chemical hardness (see below) and to check it against the form derived from combined eqs. (4) and (7).

2.2. Chemical Hardness of Atoms in Molecule

For the atoms in molecules chemical hardness computing, one may consider its inverse connection with chemical softness [18, 26]

$$S = \frac{1}{2\eta} \tag{9}$$

since the advantage of evaluating the propensity to reactivity than the resistance to it. As such, for a multi-atomic system the chemical bond is appropriately represented by the direct overlapping of all involved atomic electronic clouds' deformations (directly related to softness), yielding the molecular softness simply as [27]

$$S_M = \sum_A S_A \tag{10}$$

On the other hand, each of the AIM softness in eq. (10) is contributing to the molecular one through a specific index of reactivity called the Fukui function (f_A) [18c, 26d]

$$S_A = f_A S_M \tag{11}$$

that measures the local modifications of the atomic frontier orbital/density toward exchanged electrons in molecule [28]

$$f_A(\mathbf{r}) = \left(\frac{\partial \rho_A(\mathbf{r})}{\partial N_A} \right)_{V_A(\mathbf{r})} = -\left(\frac{\delta \chi_A}{\delta V_A(\mathbf{r})} \right)_{N_A} \tag{12}$$

Now, when noting in eq. (12) the atomic Fukui function dependence on the functional derivative of the respective (atomic) electronegativity, in formal agreement with the chemical hardness – electronegativity relationship (5b), there appears that the atomic Fukui functions regulates the atoms-in-molecules chemical hardness by playing the role of the coefficients on the linear molecular chemical hardness expansion over the atomic contributions [18a-c, 26]

$$\eta_M = \sum_A f_A \eta_A \tag{13}$$

Eq. (13) can be further elaborated when replacing the atomic Fukui functions of eq. (11) with the help of eq. (10)

$$f_A = \frac{S_A}{\sum_A S_A} \tag{14}$$

providing the softness-hardness formulation of AIM hardness,

$$\eta_M = \frac{\sum_A S_A \eta_A}{\sum_A S_A} \tag{15}$$

that constitutes the counterpart AIM hardness equation for what eq. (3) represented for AIM electronegativity. However, there are two major differences: (i) it is directly

obtained in the generalized poly-atomic form; and (ii) it couples at nominator the softness and hardness reactivity indices belonging to the same atom in molecule, and unmixed atomic terms as previously noted. At the same time, the denominator of eq. (15) reaffirms the already pointed fact that chemical hardness approaches a maximum value when the chemical bond is stabilized/optimized among the adducts. This is here confirmed by the natural necessity the molecular softness (10) is minimum in (15), since modeling the minimum overlap of the atomic frontier orbitals of the participating atoms in bonding. This is also natural since the chemical bonding is seen as a perturbation in atomic configuration when entering a molecular combination so that only the valence region is affected, and not the core level (that would be nevertheless impeded by the nuclear reciprocal repulsion). Thus, also the softness approach accords with maximum hardness principle of reactivity and bonding.

Finally, when softness-chemical hardness transformation (9) counts in eq. (15) it produces the working formula for AIM chemical hardness

$$\eta_{AIM} = \frac{n_{AIM}}{\sum_{A} \frac{n_A}{\eta_A}} \tag{16}$$

which happens to have the same analytical form as that found for the AIM electronegativity, see eq. (7). At this point, one could say that since the eq. (16) may be directly derived through applying the transformation (4) upon the electronegativity result (7) they should both be valid and appropriate for further applications.

Nevertheless, it is obvious that AIM chemical hardness and electronegativity, although somehow related, may be regarded as different (complementary) approaches of reactivity, a matter that will also be studied with regard to the aromaticity concept.

2.3. Compact Finite Difference for Electronegativity and Chemical Hardness

Beside the atoms-in-molecule approach, it is possible to express directly molecular electronegativity and chemical hardness by employing their basic formulations (1) and (2) by their approximation as compact finite differences. This procedure uses the molecular frontier orbitals and is based on differential expansion of the energy around its isolated value to account both for the electrophilic (electrons accepting) and nucleophilic (electrons donating) states.

Actually, when the parabolic form of the energy vs. electronic number dependency is assumed [17c, 18c], the derivatives of eqs. (1) and (2) may be accurately evaluated through considering the states with *N*-3, *N*-2, *N*-1, *N*+1, *N*+2, *N*+3 electrons, whereas the derivatives in the neighbor states will be taken only as their most neighboring dependency. This way, the working formulas for electronegativity will be:

$$-\chi = \frac{\partial E}{\partial N}\Big|_{|N\rangle}$$

$$\cong a_1 \frac{E_{N+1} - E_{N-1}}{2} + b_1 \frac{E_{N+2} - E_{N-2}}{4} + c_1 \frac{E_{N+3} - E_{N-3}}{6}$$

$$-\alpha_1\left(\frac{\partial E}{\partial N}\Big|_{|N-1\rangle} + \frac{\partial E}{\partial N}\Big|_{|N+1\rangle}\right) - \beta_1\left(\frac{\partial E}{\partial N}\Big|_{|N-2\rangle} + \frac{\partial E}{\partial N}\Big|_{|N+2\rangle}\right)$$

$$= a_1 \frac{E_{N+1} - E_{N-1}}{2} + b_1 \frac{E_{N+2} - E_{N-2}}{4} + c_1 \frac{E_{N+3} - E_{N-3}}{6}$$

$$-\alpha_1\left(a_1 \frac{E_N - E_{N-2}}{2} + a_1 \frac{E_{N+2} - E_N}{2}\right) - \beta_1\left(a_1 \frac{E_{N-1} - E_{N-3}}{2} + a_1 \frac{E_{N+3} - E_{N+1}}{2}\right)$$

$$= a_1(1+\beta_1)\frac{E_{N+1} - E_{N-1}}{2} + (b_1 - 2a_1\alpha_1)\frac{E_{N+2} - E_{N-2}}{4} + (c_1 - 3a_1\beta_1)\frac{E_{N+3} - E_{N-3}}{6} \quad (17)$$

and respectively for the chemical hardness as [20c]

$$2\eta = \frac{\partial^2 E}{\partial N^2}\Big|_{|N\rangle}$$

$$\cong 2a_2 \frac{E_{N+1} - 2E_N + E_{N-1}}{2} + b_2 \frac{E_{N+2} - 2E_N + E_{N-2}}{4} + c_2 \frac{E_{N+3} - 2E_N + E_{N-3}}{9}$$

$$-\alpha_2\left(\frac{\partial^2 E}{\partial N^2}\Big|_{|N-1\rangle} + \frac{\partial^2 E}{\partial N^2}\Big|_{|N+1\rangle}\right) - \beta_2\left(\frac{\partial^2 E}{\partial N^2}\Big|_{|N-2\rangle} + \frac{\partial^2 E}{\partial N^2}\Big|_{|N+2\rangle}\right)$$

$$= 2a_2 \frac{E_{N+1} - 2E_N + E_{N-1}}{2} + b_2 \frac{E_{N+2} - 2E_N + E_{N-2}}{4} + c_2 \frac{E_{N+3} - 2E_N + E_{N-3}}{9}$$

$$-\alpha_2\left(2a_2 \frac{E_N - 2E_{N-1} + E_{N-2}}{2} + 2a_2 \frac{E_{N+2} - 2E_{N+1} + E_N}{2}\right)$$

$$-\beta_2\left(2a_2 \frac{E_{N-1} - 2E_{N-2} + E_{N-3}}{2} + 2a_2 \frac{E_{N+3} - 2E_{N+2} + E_{N+1}}{2}\right)$$

$$= 2a_2(1 + 2\alpha_2 - \beta_2)\frac{E_{N+1} + E_{N-1}}{2} + (8a_2\beta_2 + b_2 - 4a_2\alpha_2)\frac{E_{N+2} + E_{N-2}}{4}$$

$$+\left(c_2-9a_2\beta_2\right)\frac{E_{N+3}+E_{N-3}}{9}-\left(2a_2+\frac{1}{2}b_2+\frac{2}{9}c_2+2a_2\alpha_2\right)E_N \qquad (18)$$

where the involved parameters discriminate between various schemes of computations and the spectral-like resolution (SLR), see Table 1 [20c, 29, 30].

Next, the eqs. (17) and (18) may be rewritten in terms of the observational quantities, as the ionization energy and electronic affinity are with the aid of their basic definitions from the involved eigen-energies of *i*-th (*i*=1,2,3) order

$$I_i = E_{N-i} - E_{N-i+1} \qquad (19a)$$

$$A_i = E_{N+i-1} - E_{N+i} \qquad (19b)$$

As such they allow the energetic equivalents for the differences

$$E_{N+1} - E_{N-1} = -(I_1 + A_1) \qquad (20a)$$

$$E_{N+2} - E_{N-2} = -(I_1 + A_1) - (I_2 + A_2) \qquad (20b)$$

$$E_{N+3} - E_{N-3} = -(I_1 + A_1) - (I_2 + A_2) - (I_3 + A_3) \qquad (20c)$$

and for the respective sums [20c]

$$E_{N+1} + E_{N-1} = (I_1 - A_1) + 2E_N \qquad (21a)$$

$$E_{N+2} + E_{N-2} = (I_1 - A_1) + (I_2 - A_2) + 2E_N \qquad (21b)$$

$$E_{N+3} + E_{N-3} = (I_1 - A_1) + (I_2 - A_2) + (I_3 - A_3) + 2E_N \qquad (21c)$$

being then implemented to provide the associate "spectral" molecular analytical forms of electronegativity

$$\chi_{CFD} = \left[a_1\left(1-\alpha_1\right)+\frac{1}{2}b_1+\frac{1}{3}c_1\right]\frac{I_1+A_1}{2}$$
$$+\left[b_1+\frac{2}{3}c_1-2a_1\left(\alpha_1+\beta_1\right)\right]\frac{I_2+A_2}{4}$$
$$+\left(c_1-3a_1\beta_1\right)\frac{I_3+A_3}{6} \qquad (22)$$

and for chemical hardness [20c]:

$$\eta_{CFD} = \left[a_2(1-\alpha_2+2\beta_2)+\frac{1}{4}b_2+\frac{1}{9}c_2\right]\frac{I_1-A_1}{2}$$
$$+\left[\frac{1}{2}b_2+\frac{2}{9}c_2+2a_2(\beta_2-\alpha_2)\right]\frac{I_2-A_2}{4}$$
$$+\left[\frac{1}{3}c_2-3a_2\beta_2\right]\frac{I_3-A_3}{6} \qquad (23)$$

Table 1. *Numerical parameters for the compact finite second (2C)-, fourth (4C)- and sixth (6C)-order central differences; standard Padé (SP) schemes; sixth (6T)- and eight (8T)-order tridiagonal schemes; eighth (8P)- and tenth (10P)- order pentadiagonal schemes up to spectral-like resolution (SLR) schemes for the electronegativity and chemical hardness of Eqs. (17) and (18) and the subsequent of their respective formulations: eqs. (22) and (23); (27) and (28) [20c, 29, 30].*

Scheme	Electronegativity					Chemical Hardness				
	a_1	b_1	c_1	α_1	β_1	a_2	b_2	c_2	α_2	β_2
2C	1	0	0	0	0	1	0	0	0	0
4C	$\frac{4}{3}$	$-\frac{1}{3}$	0	0	0	$\frac{4}{3}$	$-\frac{1}{3}$	0	0	0
6C	$\frac{3}{2}$	$-\frac{3}{5}$	$\frac{1}{10}$	0	0	$\frac{12}{11}$	$\frac{3}{11}$	0	$\frac{2}{11}$	0
SP	$\frac{5}{3}$	$\frac{1}{3}$	0	$\frac{1}{2}$	0	$\frac{6}{5}$	0	0	$\frac{1}{10}$	0
6T	$\frac{14}{9}$	$\frac{1}{9}$	0	$\frac{1}{3}$	0	$\frac{3}{2}$	$-\frac{3}{5}$	$\frac{1}{5}$	0	0
8T	$\frac{19}{12}$	$\frac{1}{6}$	0	$\frac{3}{8}$	0	$\frac{147}{152}$	$\frac{51}{95}$	$-\frac{23}{760}$	$\frac{9}{38}$	0
8P	$\frac{40}{27}$	$\frac{25}{54}$	0	$\frac{4}{9}$	$\frac{1}{36}$	$\frac{320}{393}$	$\frac{310}{393}$	0	$\frac{344}{1179}$	$\frac{23}{2358}$
10P	$\frac{17}{12}$	$\frac{101}{150}$	$\frac{1}{100}$	$\frac{1}{2}$	$\frac{1}{20}$	$\frac{1065}{1798}$	$\frac{1038}{899}$	$\frac{79}{1798}$	$\frac{334}{899}$	$\frac{43}{1798}$
SLR	1.303	0.994	0.038	0.577	0.09	0.216	1.723	0.177	0.502	0.056

It is worth remarking that when particularizing these formulas for the fashioned two-point central finite difference, i.e. when having $a_1 = 1, b_1 = c_1 = \alpha_1 = \beta_1 = 0$ and $a_2 = 1, b_2 = c_2 = \alpha_2 = \beta_2 = 0$ of Table 1, one recovers the consecrated Mulliken (spectral) electronegativity [31]

$$\chi_{2C} = \frac{I_1 + A_1}{2} \tag{24}$$

and the chemical hardness basic form relating with the celebrated Pearson nucleophilic-electrophilic reactivity gap [18a-c]

$$\eta_{2C} = \frac{I_1 - A_1}{2} \tag{25}$$

already used as measuring the aromaticity through the molecular stability against the reaction propensity [15c, 19].

Finally, for computational purposes, formulas (22) and (23) may be once more reconsidered within the Koopmans' frozen core approximation [32], in which various

orders of ionization potentials and electronic affinities are replaced by the corresponding frontier energies

$$I_i = -\varepsilon_{HOMO(i)} \tag{26a}$$

$$A_i = -\varepsilon_{LUMO(i)} \tag{26b}$$

so that the actual working compact finite difference (CFD) orbital molecular electronegativity unfolds as

$$\chi_{CFD} = -\left[a_1\left(1-\alpha_1\right)+\frac{1}{2}b_1+\frac{1}{3}c_1\right]\frac{\varepsilon_{HOMO(1)}+\varepsilon_{LUMO(1)}}{2}$$

$$-\left[b_1+\frac{2}{3}c_1-2a_1\left(\alpha_1+\beta_1\right)\right]\frac{\varepsilon_{HOMO(2)}+\varepsilon_{LUMO(2)}}{4}$$

$$-\left(c_1-3a_1\beta_1\right)\frac{\varepsilon_{HOMO(3)}+\varepsilon_{LUMO(3)}}{6} \tag{27}$$

along with the respective chemical hardness formulation [20c]

$$\eta_{CFD} = \left[a_2\left(1-\alpha_2+2\beta_2\right)+\frac{1}{4}b_2+\frac{1}{9}c_2\right]\frac{\varepsilon_{LUMO(1)}-\varepsilon_{HOMO(1)}}{2}$$

$$+\left[\frac{1}{2}b_2+\frac{2}{9}c_2+2a_2\left(\beta_2-\alpha_2\right)\right]\frac{\varepsilon_{LUMO(2)}-\varepsilon_{HOMO(2)}}{4}$$

$$+\left[\frac{1}{3}c_2-3a_2\beta_2\right]\frac{\varepsilon_{LUMO(3)}-\varepsilon_{HOMO(3)}}{6} \tag{28}$$

Note that the actual CFD electronegativity and chemical hardness expressions do not distinguish for the atoms-in-molecule contributions, while providing post-bonding information and values, i.e. for characterizing the already stabilized/optimized molecular structure towards its further reactive engagements. The difference between the atoms-in-molecule pre-bonding stage and the molecular post-bonding one constitutes the basis of the actual absolute aromaticity as it will be next introduced.

2.4. Absolute Aromaticity

Having clarified the atoms-in-molecule and (frontier) molecular orbital-based methods for computing the molecular electronegativity and chemical hardness, one can infer that they represent two different stages in bonding. This way, while the superposition of atoms in molecule belongs to the bond forming stage, being mostly dominated by their reciprocal attraction – driven by electronegativity equalization

principle of atoms in molecule [24], the reactivity based on the frontier orbitals, i.e. HOMO and LUMO states in different orders, merely addresses the post-bonding molecular stability that is governed by the maximum hardness principle [21].

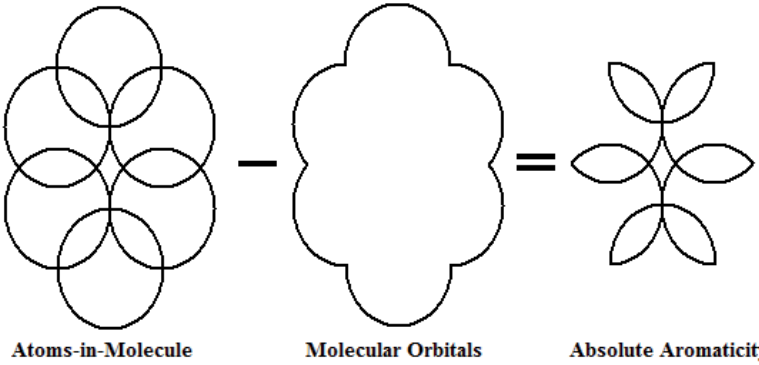

Figure 1. *Heuristic representation of the concept of absolute aromaticity (for the benzene pattern) as the stabilization difference of a given index of reactivity between atoms-in-molecule and molecular orbitals bonding configurations.*

Now, it seems natural to compare the two stages of a molecular bonding, for a given reactivity index, which through their difference should reveal the excess chemical information responsible for the stability of that molecular system. In other words, by subtracting the already formed molecular orbital (MO) information Π_{MO} from that obtained by superposition of atomic information in bonding Π_{AIM}

$$A = \Pi_{AIM} - \Pi_{MO} \tag{29}$$

one yields the chemical information that characterizes the stability of the chemical bond itself – what is presently attributed to the absolute aromaticity. The *absolute* adjective comes from the fact the aromaticity degree is obtained by employing different presumably equivalent information regarding *the same* molecule, see Figure 1 for a heuristic representation, and not by using two molecular systems – one tested and one referential as the custom definitions for the *relative* reactivity scales of aromaticity do [19].

When the electronegativity index is considered in eq. (29) the electronegativity-based absolute aromaticity is obtained with the working form

$$A^{\chi} = \chi_{AIM} - \chi_{CFD} \tag{30}$$

that in turn, can be further specialized when the AIM formulation of eq. (7) is combined with different compact finite differences schemes encompassed by the eq. (27), with the parameters given in Table 1. Regarding the aromaticity scale tendency, it will be established by appealing the electronegativity reactivity behavior. For instance, higher AIM electronegativity χ_{AIM} higher bonding propensity through the electronic flowing between atoms-in-molecule according to the electronegativity equalization principle; on the other hand, the formed molecule is as stable as posing the lower orbital molecular electronegativity χ_{CFD} that restricts its engagement in further electrophilic reactions. The result is that *higher A^{χ} is associated with higher stability and aromaticity of the envisaged system*.

Instead, when chemical hardness based absolute aromaticity is particularized out of the general definition (29) with the help of AIM and CFD eqs. (16) and (28), respectively

$$A^{\eta} = \eta_{AIM} - \eta_{CFD} \tag{31}$$

the aromaticity scale is reversed following the specific (previously presented) chemical hardness reactivity principle. That is, the formed molecular bond (orbitals) – once optimized – associate with maximum hardness η_{CFD} (otherwise the binding process will continue until the maximum hardness stabilization of the final configuration will be reached anyway); on the contrary, the atoms-in-molecule state should be characterized by non-maximum chemical hardness value η_{AIM} not to impede the bond formation towards its stabilized stereo-chemical configuration. All in all, it is clear that *as A^{η} takes lower values, it indicates more stable and aromatic systems*.

The introduced electronegativity and chemical hardness-based absolute aromaticity formulations (30) and (31) and ordering based on their chemical reactivity principles are to be in tested next for paradigmatic molecules and other aromaticity criteria.

3. Application and Discussion

Although aromaticity has neither reached a definitive formulation nor a physical-chemical criterion of orderability, the important historical contributions have

established so far the main directions a suitable scale has to be tested, namely the energetic, geometric (including topological), magnetic, and reactivity criteria.

The reactivity criteria were previously formulated when minimum electronegativity and maximum chemical hardness features for molecular stabilization against electrophilicity were considered in assessing the maximum and minimum hierarchical tendencies for the associated absolute aromaticities, eqs. (30) and (31), respectively. In fact, it is this criterion that needs to be validated in comparison with the consecrated ones, described below.

The geometric (and some topological) criteria predict a more aromatic compound the higher the associate index provided. This is the case of HOMA [11] and TOPAZ [14] indices that for increased values assess the compound with more aromatic conjugated ring or molecular fragment/zone, paralleling the more delocalized π-electrons in question. Instead, the reverse hierarchy is assumed for the recent topological index of reactivity (TIR) that, since related with the molecular site where the maximum probability (entropy) in electrophilic substitution (i.e. destabilization of the aromatic ring or system) takes place, recommending lower values for higher aromaticity [15c].

The energetic criterion of aromaticity is a classical one originating in the works of Pauling and Wheland [33], and is based on the resonance energy (RE) concept that was somehow twisted towards the difference between the π-electronic delocalization respecting a reference π-system without delocalization [34]; when reported per concerned π-electrons (PE) yields the REPE index [35] of whose magnitude estimates the stabilization energy and therefore the aromaticity degree [36]; in short: the higher REPE, the higher aromaticity is predicted. Closely related with the resonance energy is the thermodynamic stabilization criterion of energy: the more stable a structure is, the lower its heat (enthalpy) of formation $\Delta_f H^0$. Quantitatively, the molecular heat of formation may be evaluated by the atoms-in-molecule equation

$$\Delta_f H^0_{\text{molecule}} = E_{\text{binding}} - \sum \Delta_f H^0_{\text{atom}} \qquad (32)$$

by subtracting atomic heats of formation from the molecule's binding energy; In this regard, the heat of formation definition (32) and criterion parallel the chemical hardness-based absolute aromaticity index (31) phenomenology. It is therefore a useful measure for aromaticity and will be investigated next to complete the chemical

reactivity criteria. However, the practical quantum computations of these quantities is made by the semi-empirical methods based on neglecting of the differential (diatomic) overlapping (NDO) [37], especially the modified intermediate NDO (MINDO) [38], MNDO/3 [39], Austin Model (AM1) [40], and parameterized model no. 3 (PM3) [41] algorithms that are parameterized by fitting to experimentally determined heats (enthalpies) of formation for a set of molecules at 298 K. Yet, since for most organic molecules, AM1 reports heats of formation accurate to within a few kilocalories per mol respecting those experimentally measured [42] it will be assumed as the present computational framework in furnishing the heats of formation for the actual working set of molecules.

The magnetic property belongs to the physical interpretation of aromaticity and is modulated by two popular indices. Once is the nucleus-independent chemical shift (NICS) index [43] that correlates the higher π-delocalization with the increasing of magnetization (vector) in the center of the aromatic ring (or at other concerned point of the system); consequently, the larger magnetization, the larger aromaticity will be. Instead, the exaltation of magnetic susceptibility [44], measuring the resistance to magnetization introduces the index (Λ) that takes lower values for higher stability and aromaticity, being usually reported as an extensive quantity, i.e. it is calculated per π-electron, as it is also the case with REPE index.

The HOMA, TOPAZ, TIR, REPE, $\Delta_f H^0$ and Λ indices and their aromatic scales for a series of representative benzenoid hydrocarbons are presented in Table 2 [15c, 35]. In order to compare them with the actual electronegativity and chemical hardness-based absolute aromaticities the AIM electronegativity and chemical hardness values are first computed and reported in Table 2 based on eqs. (7) and (16), respectively; then, they were combined with the CFD counterparts for all schemes from Table 1 applied on eqs. (27) and (28) through employing the semi-empirical AM1 quantum mechanically calculation of the involved frontier orbitals and energies [45]; the resulted absolute aromaticities are presented in Tables 3 and 4, respectively.

For a better visualization of the trends and particularities of the various absolute aromatic scales computed along the whole plethora of compact finite differences of electronegativity and chemical hardness, their linear correlations with the considered geometric, topologic, energetic, and magnetic aromatic scales are performed - with the correlation coefficients reported in Table 5. Table 5 furnishes

very interesting information on compatible aromatic scales as well as on electronegativity and chemical hardness behavior against aromaticity.

Table 2. *Aromaticity values for common benzenoid molecules by means of the HOMA [15c], Topological Paths and Aromatic Zones - TOPAZ [30], topological index of reactivity -TIR [15c], resonance energy per π-electron – REPE (×10³[β]) [35], the heats (enthalpies) of formations $\Delta_f H^0$ [kcal/mol] at 298 K computed within semi-empirical AM1 method [45], and exaltation magnetic susceptibility Λ [cgs-ppm] [15c] methods, along the atoms-in-molecule (AIM) electronegativity and chemical hardness values (in electron-Volts [eV]) computed upon eqs. (7) and (16), respectively, based on the constituting atomic values (χ_H=7.18eV; χ_C=6.24eV; η_H=6.45eV; η_C=4.99eV) [17d].*

No.	Molecule		A_{HOMA}	A_{TOPAZ}	A_{TIR}	A_{REPE}	$\Delta_f H^0$	A_Λ	χ_{AIM}	η_{AIM}
	Name	AIM								
1	Benzene	C_6H_6	0.991	999.2	0.000	65	21.867	14.5	6.677	5.627
2	Naphthalene	$C_{10}H_8$	0.811	616.2	0.252	55	40.346	29.6	6.626	5.548
3	Anthracene	$C_{14}H_{10}$	0.718	585.0	0.571	47	62.606	45.5	6.600	5.510
4	Phenanthrene	$C_{14}H_{10}$	0.742	520.3	0.318	55	57.128	41.4	6.600	5.510
5	Pyrene	$C_{16}H_{10}$	0.742	561.2	0.585	51	67.003	59.2	6.571	5.466
6	Naphthacene	$C_{18}H_{12}$	0.670	579.4	0.638	42	86.550	62.2	6.585	5.487
7	Benz[*a*]anthracene	$C_{18}H_{12}$	0.696	522.4	0.568	50	77.853	55.2	6.585	5.487
8	Chrysene	$C_{18}H_{12}$	0.709	468.8	0.466	53	75.816	55.5	6.585	5.487
9	Triphenylene	$C_{18}H_{12}$	0.691	474.9	0.338	56	75.100	49.3	6.585	5.487
10	Perylene	$C_{20}H_{12}$	0.656	556.3	0.636	48	88.884	42.8	6.562	5.453
11	Benzo[*e*]pyrene	$C_{20}H_{12}$	0.690	501.6	0.589	53	83.569	66.9	6.562	5.453
12	Benzo[*a*]pyrene	$C_{20}H_{12}$	0.700	517.9	0.702	49	87.094	72.2	6.562	5.453
13	Pentacene	$C_{22}H_{14}$	0.644	578.7	0.739	38	111.377	79.9	6.575	5.472
14	Benzo[*a*]naphthacene	$C_{22}H_{14}$	0.660	531.4	0.631	45	101.026	70.3	6.575	5.472
15	Dibenz[*a,h*]anthracene	$C_{22}H_{14}$	0.683	482.0	0.558	51	93.725	66.6	6.575	5.472
16	Benzo[*b*]chrysene	$C_{22}H_{14}$	0.680	474.7	0.590	49	97.216	70.5	6.575	5.472
17	Picene	$C_{22}H_{14}$	0.697	444.8	0.497	53	93.866	68.6	6.575	5.472
18	Benzo[*ghi*]perylene	$C_{22}H_{12}$	0.707	502.0	0.629	51	90.866	79.8	6.542	5.423
19	Anthanthrene	$C_{22}H_{12}$	0.691	572.1	0.712	45	98.970	89.3	6.542	5.423
20	Naphtho[2,1,8-*qra*]naphthacene	$C_{24}H_{14}$	0.665	519.0	0.707	45	109.144	85.7	6.556	5.444
21	Benzo[*a*]perylene	$C_{24}H_{14}$	0.639	531.6	0.761	45	116.986	62.3	6.556	5.444
22	Benzo[*b*]perylene	$C_{24}H_{14}$	0.642	514.0	0.656	49	106.444	56.0	6.556	5.444
23	Coronene	$C_{24}H_{12}$	0.742	471.8	0.557	53	95.751	123.9	6.525	5.397
24	Zethrene	$C_{24}H_{14}$	0.623	581.9	0.759	41	116.923	45.5	6.556	5.444
25	Benzo[*a*]pentacene	$C_{26}H_{16}$	0.638	476.7	0.716	42	125.431	86.7	6.568	5.461
26	Dibenzo[*b,k*]chrysene	$C_{26}H_{16}$	0.661	476.2	0.579	46	118.894	85.9	6.568	5.461
27	Naphtho[2,3-*g*]chrysene	$C_{26}H_{16}$	0.657	451.4	0.616	51	131.680	76.2	6.568	5.461
28	Naphtho[8,1,2-*bcd*]perylene	$C_{26}H_{14}$	0.661	526.2	0.702	47	115.652	71.9	6.540	5.419
29	Dibenzo[*cd,lm*]perylene	$C_{26}H_{14}$	0.690	502.8	0.720	48	115.774	105.1	6.540	5.419
30	Dibenzo[*a,f*]perylene	$C_{28}H_{16}$	0.630	533.3	0.837	43	176.147	81.1	6.552	5.438
31	Phenanthro[1,10,9,8-*opqra*]perylene	$C_{28}H_{14}$	0.600	565.1	0.879	42	134.430	58.2	6.525	5.397
32	Dibenzo[*de,op*]pentacene	$C_{28}H_{16}$	0.620	602.0	0.856	38	144.619	48.4	6.552	5.438
33	Dibenzo[*a,l*]pentacene	$C_{30}H_{18}$	0.637	511.5	0.699	44	139.686	94.5	6.562	5.453
34	Benzo[2,1-*a*:3,4,-*a*']dianthracene	$C_{30}H_{18}$	0.618	466.0	0.563	47	145.036	88.6	6.562	5.453
35	Naphtho[2,1,8-*yza*]hexacene	$C_{32}H_{18}$	0.636	532.5	0.790	40	157.696	116.5	6.549	5.433

It is obvious that electronegativity-based aromaticity A^{χ}_{CFD} poorly correlates with almost all traditional aromaticity scales and criteria, except with the magnetic susceptibility exaltation based aromaticity; the fascinating point here is that the best correlation of A_Λ with electronegativity absolute aromaticity parallels its poorest correlation with chemical hardness absolute aromaticity – an observation that couples the magnetization phenomenon with the electronegativity action – not surprising since

both rely on frontier electrons of the valence shells or orbitals. Moreover, this correlation with electronegativity-based absolute aromaticity is obtained within its simple Mulliken form of eq. (24) – reaffirming this electronegativity scale as the most reliable for aromaticity modeling among all available CFD.

However, the representations in Figure 2 help us understand the reciprocal A_Λ and A^{χ}_{2C} aromaticity features; on the top side it is clear that, when represented on a common scale electronegativity-based aromaticity appears merely as an average of the A_Λ scale, leading to the idea that it best describes half of the total spin aromaticity; this is further confirmed by the bottom scatter plot of Figure 2 in which, by employing the correlation factor ($R = 0.726$) to its statistical representability it turns out that $R^2 \times 100(\%) = 52.71\%$ (i.e. practically a half!) of the total variance of magnetic susceptibility exaltation is explained by its linear dependency with A^{χ}_{2C} scale.

Table 3. *Electronegativity-based absolute aromaticity values of eq. (30) by means of the combined atoms-in molecule reactivity with the various compact finite differences schemes in Table 1 for the molecules in Table 2 within AM1 semi-empirical computational framework [45]. All values in electron-Volts [eV].*

No.	A^{χ}_{2C}	A^{χ}_{4C}	A^{χ}_{6C}	A^{χ}_{SP}	A^{χ}_{6T}	A^{χ}_{8T}	A^{χ}_{8P}	A^{χ}_{10P}	A^{χ}_{SLR}
1	2.127	2.107	2.097	5.097	3.777	4.077	4.157	4.177	3.947
2	2.136	2.156	2.156	5.196	3.846	4.146	4.236	4.256	4.006
3	2.120	2.140	2.150	5.190	3.840	4.150	4.220	4.240	3.990
4	2.090	2.090	2.090	5.120	3.780	4.080	4.170	4.180	3.940
5	2.061	2.061	2.061	5.091	3.751	4.051	4.141	4.151	3.911
6	2.075	2.085	2.095	5.135	3.785	4.095	4.175	4.185	3.935
7	2.095	2.125	2.125	5.225	3.855	4.165	4.265	4.295	4.055
8	2.065	2.075	2.075	5.115	3.765	4.065	4.145	4.165	3.915
9	2.025	2.035	2.035	5.105	3.745	4.045	4.135	4.155	3.905
10	2.062	2.082	2.092	5.172	3.802	4.112	4.192	4.202	3.952
11	2.022	2.032	2.032	5.082	3.722	4.032	4.112	4.132	3.892
12	2.042	2.062	2.062	5.112	3.762	4.062	4.142	4.162	3.912
13	2.075	2.075	2.075	5.105	3.765	4.065	4.155	4.165	3.925
14	2.065	2.065	2.075	5.125	3.765	4.075	4.155	4.165	3.915
15	2.045	2.055	2.055	5.095	3.745	4.055	4.135	4.145	3.895
16	2.055	2.065	2.065	5.115	3.755	4.065	4.145	4.165	3.905
17	2.035	2.045	2.045	5.095	3.745	4.045	4.125	4.145	3.895
18	2.002	2.002	2.002	5.062	3.702	4.012	4.092	4.112	3.862
19	2.012	2.032	2.042	5.102	3.742	4.052	4.132	4.142	3.892
20	2.036	2.046	2.046	5.096	3.746	4.046	4.126	4.146	3.896
21	2.046	2.046	2.046	5.026	3.706	4.006	4.076	4.096	3.846
22	2.036	2.046	2.046	5.096	3.746	4.056	4.136	4.156	3.906
23	1.945	1.835	1.775	4.595	3.355	3.635	3.745	3.785	3.585
24	2.056	2.076	2.076	5.136	3.776	4.086	4.166	4.176	3.926
25	2.048	2.068	2.068	5.148	3.778	4.088	4.178	4.208	3.958
26	2.038	2.038	2.038	5.038	3.698	4.008	4.078	4.088	3.828
27	2.008	2.008	2.008	5.058	3.698	4.008	4.078	4.098	3.848
28	2.000	2.020	2.020	5.080	3.720	4.030	4.110	4.130	3.880
29	2.000	2.020	2.020	5.090	3.730	4.040	4.110	4.130	3.880
30	2.032	2.042	2.052	5.112	3.752	4.062	4.132	4.142	3.892
31	1.995	2.005	2.015	5.075	3.715	4.025	4.105	4.115	3.865
32	2.052	2.062	2.062	5.102	3.752	4.062	4.142	4.162	3.912
33	2.022	2.032	2.052	5.112	3.742	4.052	4.122	4.132	3.862
34	2.072	2.082	2.082	5.112	3.772	4.072	4.152	4.172	3.922
35	2.009	2.009	2.009	5.049	3.699	4.009	4.089	4.109	3.859

Table 4. *Chemical hardness-based absolute aromaticity values of eq. (31) by means of the combined atoms-in molecule reactivity with the various compact finite differences schemes in Table 1 for the molecules of Table 2. All values in electron-Volts [eV].*

No.	A^{η}_{2C}	A^{η}_{4C}	A^{η}_{6C}	A^{η}_{SP}	A^{η}_{6T}	A^{η}_{8T}	A^{η}_{8P}	A^{η}_{10P}	A^{η}_{SLR}
1	0.527	-0.133	1.687	1.007	-0.623	1.947	1.907	1.517	-0.043
2	1.328	0.668	2.108	1.558	0.228	2.368	2.418	2.258	1.358
3	1.870	1.340	2.610	2.130	0.980	2.810	2.820	2.630	1.730
4	1.410	0.740	2.130	1.600	0.310	2.390	2.450	2.330	1.550
5	1.366	0.696	2.086	1.546	0.266	2.336	2.406	2.286	1.506
6	1.867	1.317	2.577	2.097	0.957	2.787	2.807	2.637	1.797
7	2.227	1.797	2.947	2.507	1.477	3.117	3.107	2.877	1.957
8	1.637	1.027	2.337	1.837	0.637	2.577	2.627	2.487	1.707
9	1.387	0.757	2.167	1.637	0.347	2.417	2.447	2.267	1.357
10	2.103	1.663	2.853	2.413	1.353	3.033	3.003	2.753	1.773
11	1.773	1.193	2.453	1.973	0.823	2.673	2.723	2.583	1.803
12	2.043	1.543	2.723	2.283	1.203	2.923	2.943	2.763	1.943
13	2.482	2.082	3.142	2.742	1.812	3.302	3.282	3.072	2.222
14	2.142	1.662	2.822	2.372	1.342	3.002	3.012	2.832	2.012
15	1.742	1.152	2.412	1.932	0.772	2.642	2.692	2.572	1.842
16	1.942	1.412	2.632	2.162	1.072	2.832	2.852	2.692	1.892
17	1.652	1.032	2.322	1.832	0.642	2.562	2.622	2.512	1.802
18	1.943	1.413	2.603	2.143	1.053	2.813	2.843	2.703	1.933
19	2.293	1.863	2.973	2.553	1.573	3.133	3.123	2.923	2.073
20	2.234	1.774	2.894	2.474	1.464	3.074	3.074	2.904	2.104
21	2.354	1.964	3.074	2.654	1.684	3.224	3.194	2.944	1.984
22	2.094	1.614	2.784	2.344	1.294	2.974	2.974	2.794	1.944
23	1.797	1.247	2.487	2.007	0.877	2.697	2.727	2.567	1.767
24	2.464	2.084	3.164	2.754	1.814	3.304	3.274	3.034	2.094
25	2.411	1.991	3.071	2.661	1.701	3.231	3.221	3.021	2.161
26	2.111	1.611	2.771	2.331	1.281	2.961	2.981	2.821	2.031
27	1.881	1.321	2.551	2.081	0.961	2.761	2.801	2.671	1.931
28	2.299	1.869	2.969	2.549	1.569	3.129	3.129	2.919	2.069
29	2.359	1.929	2.999	2.599	1.629	3.169	3.169	2.979	2.159
30	2.638	2.308	3.328	2.948	2.058	3.458	3.408	3.158	2.218
31	2.687	2.377	3.367	2.997	2.137	3.487	3.437	3.177	2.247
32	2.718	2.368	3.338	2.978	2.108	3.478	3.458	3.238	2.398
33	2.333	1.893	2.983	2.573	1.593	3.153	3.153	2.973	2.163
34	1.933	1.393	2.603	2.143	1.043	2.813	2.843	2.693	1.913
35	2.583	2.173	3.163	2.783	1.893	3.323	3.333	3.173	2.453

Table 5. *Correlation coefficients for linear regressions of all aromaticity scales in Table 2 (as dependent variables) with those in Tables 3 and 4 for electronegativity and chemical hardness-based ones (as independent variables), respectively.*

X \ Y		A_{HOMA}	A_{TOPAZ}	A_{TIR}	A_{REPE}	$\Delta_f H^0$	A_A
A^{χ}	A^{χ}_{2C}	**0.441**	**0.503**	**0.520**	**0.215**	**0.548**	**0.726**
	A^{χ}_{4C}	0.212	0.356	0.313	0.056	0.386	0.697
	A^{χ}_{6C}	0.119	0.312	0.224	0.019	0.301	0.659
	A^{χ}_{SP}	0.054	0.165	0.056	0.106	0.142	0.544
	A^{χ}_{6T}	0.035	0.242	0.139	0.054	0.225	0.608
	A^{χ}_{8T}	0.002	0.228	0.101	0.085	0.189	0.589
	A^{χ}_{8P}	0.030	0.234	0.135	0.061	0.235	0.606
	A^{χ}_{10P}	0.049	0.229	0.154	0.037	0.252	0.604
	A^{χ}_{SLR}	0.120	0.281	0.209	0.015	0.320	0.638
A^{η}	A^{η}_{2C}	0.846	0.383	0.941	**0.904**	0.829	0.489
	A^{η}_{4C}	0.823	0.333	0.933	0.897	0.823	0.465
	A^{η}_{6C}	0.786	0.256	0.912	0.889	0.805	0.419
	A^{η}_{SP}	0.802	0.286	0.921	0.892	0.813	0.436
	A^{η}_{6T}	0.822	0.328	0.932	0.896	0.822	0.463
	A^{η}_{8T}	0.794	0.271	0.915	0.892	0.808	0.424
	A^{η}_{8P}	0.822	0.328	0.929	0.901	0.819	0.455
	A^{η}_{10P}	0.872	0.452	**0.945**	0.901	**0.833**	0.518
	A^{η}_{SLR}	**0.909**	**0.663**	0.910	0.846	0.798	**0.604**

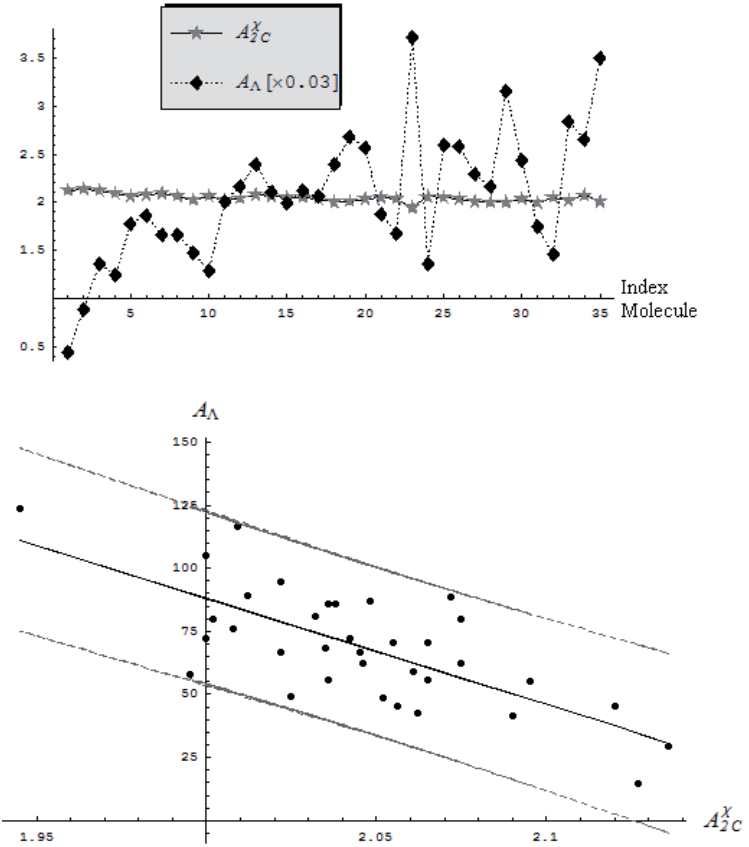

Figure 2. *Upper panel: Comparative trends of the (rescaled) magnetic susceptibility exaltation-based aromaticity (A_Λ) scale with that based on 2C finite difference scheme of electronegativity (A^{χ}_{2C}) for the molecules' information of Tables 2 and 3, respectively. Bottom panel: The statistical fit (inner line) of the linear correlation $A_\Lambda = f(A^{\chi}_{2C})$, while emphasizing on the 95% confidence interval (within the extreme lines) for the aromaticity scales of the upper panel.*

On the other hand, it is obvious that even for A^{χ}_{2C} the earlier enounced higher value for higher aromaticity criterion is not respected at the level of benzene-naphthalene couple in Table 3, as it should be, as recommended by all other aromaticity scales in Table 2. Therefore, electronegativity does not seem the proper concept for treating the absolute aromaticity, maybe because involving the form (7) based on the somehow too drastic gauge transformation (4) between AIM

electronegativity and chemical hardness, leaving with not sufficiently acceptable degree of correlation of the first with the available physicochemical aromaticity criteria.

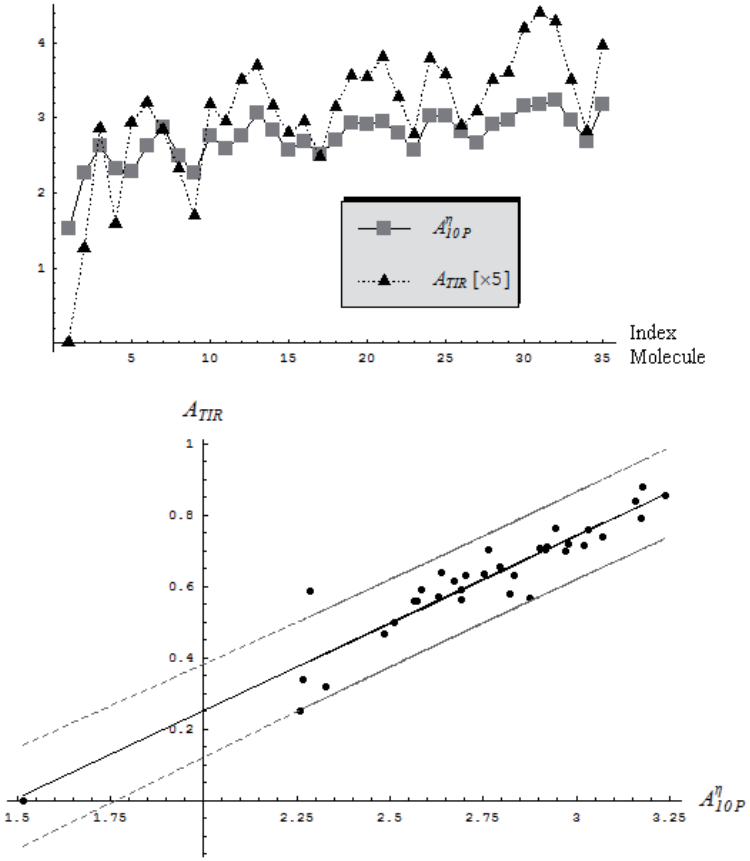

Figure 3. *The same type of representations as those in Figure 2, here for the (rescaled) topological index of reactivity-based aromaticity (A_{TIR}) versus that based on 10P finite difference scheme of chemical hardness (A^{η}_{10P}) for the molecules in Tables 2 and 4, respectively.*

The situation changes when chemical hardness-based absolute aromaticity is considered through combining the AIM chemical hardness with the molecular orbital CFD schemes in definition (31); it provides from the beginning the correct benzene-

naphthalene ordering for all computed CFD scales in Table 4 as predicted by the aromaticity criteria for the scales in Table 2; general good correlations with geometric HOMA and energetic REPT and $\Delta_f H^0$ scales, excellent correlation with TIR index (with correlation factors over 0.9 for all compact finite difference schemes), while surprisingly poor correlation with TOPAZ aromaticity and anticipated poor correlation with A_Λ scale are revealed in Table 5. While the poor correlations $A_\Lambda=f(A^\eta_{CFD})$ are explained since compensated by the superior companion electronegativity-based aromaticity correlations in Table 5, the poor correlations $A_{TOPAZ}=f(A^\eta_{CFD})$ may rely on the insufficient information that chemical hardness contains in order to be properly mapped into the generalized conjugated circuits that count in TOPAZ aromaticity algorithm [14]; the proof for the improvement of this situation when other structural indices are added into correlation has been recently given by Tarko and Putz, showing that the best correlation was obtained either when higher orders of CFD electronegativity and chemical hardness schemes are considered together or when chemical hardness is accompanied by the index of maximum aromaticity of aromatic chemical bonds and by the total accessibility index weighted by atomic masses [30].

Turning to the good correlations of the actual A^η_{CFD} scales, one may see that the highest order of CFD scheme, i.e. the spectral-like resolution chemical hardness-based aromaticity index A^η_{SLR} is in best agreement with HOMA aromaticity, while the simpler scheme, i.e. the electrophilicity-nucleophilicity chemical hardness gap (25), based aromaticity index A^η_{2C} is best correlating with REPE aromaticity. Both of these fits are motivated: the A_{HOMA} and A^η_{SLR} indices practically parallel geometrical molecular optimization with the most complex frontier orbitals' involvement – thus both accounting for the stereochemical control [46], while A_{REPE} and A^η_{2C} correlate well in the virtue of the fact that the resonance stabilization may be sufficiently modeled by the first order of the HOMO-LUMO gap.

It remains to comment upon the overall best correlation found between the TIR aromaticity and with that not based on the most complicated chemical hardness CFD-SLR scheme, but with that immediately before it, namely with the A^η_{10P} scale in Table 4. Note that the same absolute aromaticity scale A^η_{10P} is found as having the highest degree of correlation with heats of formation among all CFD-chemical hardness schemes of computation, although not with the highest correlation factor

among all others aromaticity dependent indices in Table 5. For the $A_{TIR}(A^{\eta}_{10P})$ correlation the almost perfect parallel trend among all the molecules in Table 2 is emphasized on the top plot of Figure 3, while in its bottom representation the confidence interval of their scatter plot is shown. It is worth remarking that the fine agreement of A_{TIR} index with A^{η}_{10P} index in special and with A^{η}_{CFD} schemes in general originates in the fact that all these scales of aromaticity are computed in an absolute manner, i.e. restricting the information contained within the concerned molecule without appealing to any other reference molecular system or property.

Table 6. *Correlation coefficients for linear regressions of all electronegativity-based aromaticity scales in Table 3 (as dependent variables) respecting those of chemical hardness- based aromaticity scales in Table 4 (as independent variables).*

X \ Y	A^{χ}_{2C}	A^{χ}_{4C}	A^{χ}_{6C}	A^{χ}_{SP}	A^{χ}_{6T}	A^{χ}_{8T}	A^{χ}_{8P}	A^{χ}_{10P}	A^{χ}_{SLR}
A^{η}_{2C}	0.428	0.222	0.140	0.020	0.060	0.022	0.049	0.061	0.115
A^{η}_{4C}	0.416	0.214	0.134	0.023	0.054	0.016	0.044	0.056	0.108
A^{η}_{6C}	0.375	0.180	0.102	0.046	0.026	0.011	0.017	0.029	0.078
A^{η}_{SP}	0.392	0.192	0.113	0.039	0.035	0.002	0.026	0.038	0.088
A^{η}_{6T}	0.416	0.214	0.133	0.023	0.053	0.016	0.044	0.056	0.108
A^{η}_{8T}	0.376	0.179	0.101	**0.048**	0.024	0.013	0.015	0.027	0.076
A^{η}_{8P}	0.396	0.193	0.113	0.041	0.035	0.003	0.025	0.037	0.088
A^{η}_{10P}	0.438	0.225	0.143	0.021	0.061	0.023	0.050	0.062	0.119
A^{η}_{SLR}	**0.496**	**0.281**	**0.199**	0.028	**0.117**	**0.082**	**0.105**	**0.117**	**0.179**

Remarkably, aiming to systematize somehow the aromaticity criteria against the chemical hardness-based absolute aromaticity AIM-CFD scales one can establish from Table 5 that: (i) either the topological index of reactivity A_{TIR} and the heats of formation $\Delta_f H^0$ aromaticity scales are well described by the A^{η}_{10P} absolute aromaticity index, meaning that the experimental-based heats of formation themselves may be modeled by the topological characterization of the aromatics; (ii) magnetic susceptibility exaltation A_{Λ} scale and topological paths and aromatic zones A_{TOPAZ} aromaticity index are best explained by the A^{η}_{SLR} scheme, leading to the information of their inter-correlation as well; (iii) harmonic oscillatory model-based aromaticity A_{HOMA} and the resonance energy per π-electrons A_{REPE} parallels the most complex A^{η}_{SLR} and the simplest A^{η}_{2C} schemes of chemical hardness computation in absolute aromaticity, respectively. The present results give a strong argument for further developing of aromaticity scales and criteria on an absolute basis of chemical hardness.

Finally, while remarking in the bottom plots of Figures 2 and 3 the opposite signs displayed by A_{Λ} and A_{TIR} correlations with A^{χ}_{2C} and A^{η}_{10P} scales, respectively, one likes to test whether electronegativity and chemical hardness aromaticities correlate among of their scales in Tables 3 and 4. The results reported in Table 6 show that indeed, there is practically no correlation between A^{χ}_{CFD} and A^{η}_{CFD} scales leaving us with the important idea that the electronegativity and chemical hardness indices themselves belongs to different quantum mechanically (Hilbert) spaces, or, in simple terms, are reciprocal orthogonal. Nevertheless, this is useful information to be developed in studies addressing the modeling of the chemical information and principles within the orthogonal spaces of structural quantum indices, aromaticity included.

4. Conclusions

Assessing the physical observability feature for chemical properties stands as one of the actual main issues of quantum chemistry. This happens because the main tools of basic understanding in modern conceptual and computational chemistry regard the valence, orbitals, electronegativity, chemical hardness, or the most celebrated aromaticity concepts for which no direct observed reality may be attributed. In surmounting this problem the actual theoretical research in chemistry is oriented to offer alternative or connected formulations of these concepts so that the observational character to be gained or guaranteed.

For instance, recently it was proven the electronegativity definition (1) corresponds in second quantization with the observable energies of the frontier (valence) shells of atoms and molecules [17f], a character intuitively expressed also by the Fukui function – electronegativity relationship (12). Unfortunately, for chemical hardness, a similar study is not able to definitely cut on its quantum observability [17k].

Combining these achievements with the actual study, one obtains a reliable absolute aromaticity from the chemical hardness atoms-in-molecule and compact finite difference schemes of the molecular frontier orbitals – despite their lack in assessing an undisputed quantum observable. On the other hand, when employing the observable proven electronegativity with its AIM and CFD molecular formulations

into absolutely related aromaticity poor or modest scales are obtained respecting the main geometric, topological, energetic, or magnetic criteria.

With these results it remains that aromaticity still resists embracing a fully quantum mechanical characterization. However, few constructive messages may be formulated for further developments: (i) one regards the fact that aromaticity may finely work in combination with chemical hardness in most of its forms of computation – a behavior that practically reduces the aromaticity concept and formulations to those of chemical hardness, with the remarkable achievement that the aromaticity physico-chemical scales appear to be finely regulated by the chemical hardness reactivity principles; (ii) other important realization regards the absolute definition of aromaticity that when used for chemical hardness implementation highly correlates with the topological index of reactivity [15c], absolutely defined as well – in the sense that no other information than that coming from the molecule in question is necessary – thus emphasizing the existence of a mapped information between the bonding geometry and stability/reactivity of molecules; (iii) then, the proofed reliable actual definition of absolute aromaticity viewed as the stabilization chemical information between the pre-bonding stage of atoms-in-molecule and the post-bonding stage of molecular orbitals paves the way for future studies when the similarity indices of reactivity [47] or electronic localization functions [48] are employed. They may complete the actual electronegativity and chemical hardness-based reactivity pictures of aromaticity with the help of the electronic density (observable) characterization [49].

References

[1] (a) Kekulé, A. Justus Libigs Ann Chem 1865, 137, 129; (b) Kekulé, A., Bull Acad R Belg 1865, 19, 551; (c) Kekulé, A. Bull Soc Chim Fr 1865, 3, 98.

[2] Thomson, J.J. Philos Mag 1921, 41, 510.

[3] (a) Hückel, E. Z Physik 1930, 60, 423; (b) Hückel, E. Z Physik 1931, 60, 204.

[4] Doering, W.v; Detert, F. J Am Chem Soc 1951, 73, 876.

[5] Sondheimer, F. Pure Appl Chem 1963, 7, 363.

[6] Dewar, M.S.J. Tetrahedron Suppl 1966, 8, 75.

[7] Schleyer, P.v.R.; Jiao, H. Pure Appl Chem 1996, 68, 209.

[8] Moran, D.; Simmonett, A.C.; Leach, F.E.; Allen, W.D.; Schleyer, P.v.R.; Schaeffer III, H.F. J Am Chem Soc 2006, 128, 9342.

[9] Boldyrev, A.I.; Wang, L.S. Chem Rev 2005, 105, 3716.

[10] Julg, A.; Françoise, P. Theor Chem Acta 1967, 8, 249.

[11] (a) Kruszewski, J.; Krygowski, T.M.; Tetrahedron Lett 1972, 13, 3839; (b) Krygowski, T.M. J Chem Inf Comput Sci 1993, 33, 70.

[12] (a) Randić, M. Chem Phys Lett. 1976, 38, 68; (b) Randić, M. Tetrahedron 1977, 33, 1905; (c) Randić, M. J Am Chem Soc 1977, 99, 444; (d) Gutman, I.; Milun, M.; Trinastić, N. J Am Chem Soc 1977, 99, 1692.

[13] (a) Aihara, J.; Kanno, H.; Ishida, T. J Am Chem Soc 2005, 127, 13324; (b) Aihara, J.; Kanno, H. J Mol Struct (Theochem) 2005, 722, 111.

[14] Tarko, L. Arkivoc 2008, XI, 24.

[15] (a) Balaban, A.T.; Biermann, D.; Schmidt, W. Nuov J Chim 1985, 9, 443; (b) Balaban, A.T.; Schleyer, P.v.R.; Rzepa, H.S. Chem Rev 2005, 105, 3436; (c) Ciesielski, A.; Krygowski, T.M.; Cyranski, M.K.; Dobrowolski, M.A.; Balaban, A.T. J Chem Inf Model 2009, 49, 369.

[16] McWeeny, R. Coulson's Valence, Oxford University Press, 1979, Preface.

[17] (a) Parr, R.G.; Donnelly, R.A.; Levy, M.; Palke, W.E. J Chem Phys 1978, 68, 3801; (b) Sen, K.D.; Jørgenson, C.D. (eds.) Structure and Bonding, Springer, Berlin, 1987, vol. 66; (c) Putz, M.V. Contributions within Density Functional Theory with Applications to Chemical Reactivity Theory and Electronegativity, Dissertation.com, Parkland, Florida, USA, 2003; (d) Putz, M.V. Int J Quantum Chem 2006, 106, 361; (e) Putz, M.V. J Theor Comput Chem 2007, 6, 33; (f) Putz, M.V. Int J Quantum Chem 2009, 109, 733; (k) M.V.Putz, in Quantum Frontiers of Atoms and Molecules, M.V. Putz, Ed., Nova Science Publishers, New York, 2010, Chapter 11 (in press).

[18] (a) Pearson, R.G. Chemical Hardness: Applications from Molecules to Solids, Wiley-VCH, Weinheim, 1997; (b) Sen, K.D.; Mingos, D.M.P. (Eds.) Structure and Bonding, Springer, Berlin, 1993, vol. 80; (c) Parr, R.G.; Yang, W. Density Functional Theory of Atoms and Molecules, Oxford University Press: New York, 1989; (d) Putz, M.V. Int J Mol Sci 2008, 9, 1050; (e) Putz, M.V. Absolute and Chemical Electronegativity and Hardness, Nova Science Publishers, New York, 2008.

[19] Chattaraj, P.K.; Sarkar, U.; Roy, D.R. J Chem Educ 2007, 84, 354.

[20] (a) Pearson, R.G. (ed.) Hard and Soft Acids and Bases, Dowden, Hutchinson & Ross, Stroudsberg, 1973; (b) Pearson, R.G. Coord Chem Rev 1990, 100, 403; (c) Putz, M.V.; Russo, N.; Sicilia, E. J Comput Chem 2004, 25, 994.

[21] (a) Chattaraj, P.K.; Lee, H.; Parr, R.G. J Am Chem Soc 1991, 113, 1855; (b) Chattaraj, P.K.; Schleyer, P.v.R. J Am Chem Soc 1994, 116, 1067; (c) Chattaraj, P.K.; Maiti, B.; J Am Chem Soc 2003, 125, 2705; (d) Putz, M.V. MATCH Commun Math Comput Chem 2008, 60, 845.

[22] Mandado, M.; Moa, M.J.G.; Mosquera, R.A. in Progress in Quantum Chemistry Research, E.O. Hoffman, Ed., Nova Science Publishers, New York, 2007, Chapter 1.

[23] (a) Katritzky, A.R.; Karelson, M.; Sild, S.; Krygowski, T.M.; Jug, K. J Org Chem 1998, 63, 5228; (b) Cyrański, M.K.; Krygowski, T.M.; Katritzky, A.R.; Schleyer, P.v.R. J Org Chem 2002, 67, 1333.

[24] (a) Sanderson, R.T. J Chem Educ 1988, 65, 112; (b) Mortier, W.J.; Genechten, K.v.; Gasteiger, J. J Am Chem Soc 1985, 107, 829.

[25] (a) Bratsch, S.G. J Chem Educ 1984, 61, 588; (b) Bratsch, S.G. J Chem Educ 1985, 62, 101.

[26] (a) Berkowitz, M.; Ghosh, S.K.; Parr, R.G. J Am Chem Soc 1985, 107, 6811; (b) Berkowitz, M.; Parr, R.G. J Chem Phys 1988, 88, 2554; (c) Garza, J.; Robles, J. Phys Rev A 1993, 47, 2680; (d) Baekelandt, B.G.; Cedillo, A.; Parr, R.G. J Chem Phys 1995, 103, 8548; (e) De Proft, F.; Liu, S.; Parr, R.G. J Chem Phys 1997, 107, 3000.

[27] (a) Chandrakumar, K.R.S.; Pal, S. J Phys Chem A 2002, 106, 11775; (b) idem, 5737; (c) Chandrakumar, K.R.S.; Pal, S. J Phys Chem A 2003, 107, 5755.

[28] (a) Senet, P. J Chem Phys 1996, 105, 6471; (b) Sentilkumar, K.; Ramaswamy, M.; Kolandaivel, P. Int J Quantum Chem 2001, 81, 4.

[29] Rubin, S.G.; Khosla, P.K. J Comp Phys 1977, 24, 217.

[30] Tarko, L.; Putz, M.V. J Math Chem 2010, 47, 487.

[31] Mulliken, R.S. J Chem Phys 1934, 2, 782.

[32] Koopmans, T. Physica 1934, 1, 104.

[33] (a) Pauling, L.; Wheland, G.W. J Chem Phys 1933, 1, 362; (b) Pauling, L. J Chem Phys 1933, 1, 606; (c) Wheland, G.W. The Theory of Resonance and its Application to Organic Chemistry, Wiley, New York, 1944.

[34] Truhlar, D.G. J Chem Educ 2007, 84, 781.

[35] Hess, B.A.; Schaad, L.J. J Am Chem Soc 1971, 93, 2413.

[36] (a) Schaad, L.J.; Hess, B.A. Chem Rev 2001, 101, 1465; (b) Cyrański, M.K. Chem Rev 2005, 105, 3773.

[37] Putz, M.V.; Duda-Seiman, D.; Mancaş, S.; Duda-Seiman, C.; Lacrămă, A.-M. in Advances in Quantum Chemical Bonding Structures, Putz, M.V. (Ed.), Transworld Research Network, Kerala, 2008, Chapter 15.

[38] Dewar, M.J.S.; Thiel, W. J Am Chem Soc 1977, 99, 4899.

[39] Thiel, W.; Voityuk, A. A. J Phys Chem 1996, 100, 616.

[40] (a) Dewar, M.J.S.; Zoebisch, E.G.; Healy, E.F.; Stewart, J.J.P. J Am Chem Soc 1985, 107, 3902; (b) Dewar, M.J.S.; Jie, C.; Yu., J. Tetrahedron 1993, 49, 5003; (c) Rocha, G.B.; Freire, R.O.; Simas, A.M.; Stewart, J.J.P. J Comput Chem 2006, 27, 1101.

[41] (a) Stewart, J.J.P. J Comput Chem 1989, 10, 209; (b) idem, 221; (c) Freire, R.O.; Rocha, G. B.; Simas, A.M. Chem Phys Lett 2006, 425, 138.

[42] Roux, M.V.; Temprado, M.; Chickos, J.S.; Nagano, Y. J Phys Chem Ref Data 2008, 37, 1855.

[43] (a) Schleyer, P.v.R.; Maerker, C.; Dransfeld, A.; Jiao, H.; Eikema Hommes, N.J.R.v. J Am Chem Soc 1996, 118, 6317; (b) Chen, Z.; Wannere, C.S.; Corminboeuf, C.; Puchta, R.; Schleyer, P.v.R. Chem Rev 2005, 105, 3842; (c) Feixas, F.; Matito, E.; Poater, J.; Solà, M. J Comput Chem 2008, 29, 1543; (d) Ciesielski, A.; Krygowski, T.M.; Cyrański, M.K.; Dobrowolski, M.A.; Aihara, J Phys Chem Chem Phys 2009, 11, 11447.

[44] (a) Dauben, H.J.Jr.; Wilson, J.D.; Laity, J.L. J Am Chem Soc 1968, 90, 811; (b) Dauben, H.J.Jr.; Wilson, J.D.; Laity, J.L. in Nonbenzenoid Aromatics, Snyder, J.P. (ed.) Academic Press, New York, 1971, Vol. 2; (c) Flygare, W.H. Chem Rev 1974, 74, 653.

[45] Hypercube, Inc. (2002) HyperChem 7.01 [Program package, Semiempirical, AM1, Polak-Ribier optimization procedure].

[46] Rzepa, H.S. J Chem Educ 2007, 84, 1535.

[47] (a) Carbo, R.; Arnau, M.; Leyda, L. Int J Quantum Chem 1980, 17, 1185; (b) Besalú, E.; Carbó, R.; Mestres, J.; Solà, M. Top Curr Chem 1995, 173, 31; (c) Solà, M.; Mestres, J.; Carbó, R.; Duran, M. J Am Chem Soc 1994, 116, 5909; (d) Poater, J.; Duran, M.; Solà, M. J Comput Chem 2001, 22, 1666.

[48] (a) Becke, A.D.; Edgecombe, K.E. J Chem Phys 1990, 92, 5397; (b) Silvi, B.; Savin, A. Nature (London) 1994, 371, 683; (c) Silvi, B. J Phys Chem A 2003, 107, 3081; (d) Scemama, A.; Chaquin, P.; Caffarel, M. J Chem Phys 2004, 121, 1725; (e) Putz, M.V. Int J Quantum Chem 2005, 105, 1; (f) Santos, J.C.; Andres, J.L.; Aizman, A.; Fuentealba, P. J Chem Theor Comput 2005, 1, 83.

[49] (a) Giambiagi, M.; de Giambiagi, M.S.; dos Santos, C.D.; de Figueiredo, A.P. Phys Chem Chem Phys 2000, 2, 3381; (b) Bultinck, P.; Ponec, R.; Van Damme, S. J Phys Org Chem 2005, 18, 706; (c) Fradera X.; Solà, M. J Comput Chem 2002, 23, 1347; (d) Poater, J.; Fradera, X.; Duran, M.; Solà, M. Chem-Eur J 2003, 9, 1113; (e) idem, 400; (f) Matito, E.; Poater, J.; Duran, M.; Solà, M. J Mol Struct (Theochem) 2005, 727, 165; (g) Matito, E.; Duran, M.; Solà, M. J Chem Phys 2005, 122, 014109; (h) Cioslowski, J.; Matito, E.; Solà, M. J Phys Chem A, 2007, 111, 6521.